Electrochemistry of poly(3,4-ethylenedioxythiophene)-polyaniline/Prussian blue electrochromic devices containing an ionic liquid based gel electrolyte film†

Melepurath Deepa,* Arvind Awadhia and Shweta Bhandari

Received 7th January 2009, Accepted 31st March 2009
First published as an Advance Article on the web 8th May 2009
DOI: 10.1039/b900091g

Electrochromic devices based on poly(3,4-ethylenedioxythiophene) (PEDOT) as the cathodic coloring electrode and polyaniline (PANI) or Prussian blue (PB) as the counter electrode containing a highly conductive, self-supporting, distensible and transparent polymer–gel electrolyte film encapsulating an ionic liquid, 1-butyl-1-methylpyrrolidiniumbis-(trifluoromethylsulfonyl)imide, have been fabricated. Polarization, charge transfer and diffusion processes control the electrochemistry of the functional electrodes during coloration and bleaching and these phenomena differ when PEDOT and PANI/PB were employed alternately as working electrodes. While the electrochemical impedance response shows good similitude for PEDOT and PANI electrodes, the responses of PEDOT and PB were significantly different in the PEDOT–PB device, especially during reduction of PB, wherein the overall amplitude of the impedance response is enormous. Large values of the coloration efficiency maxima of 281 $cm^2\ C^{-1}$ (λ = 583 nm) and 274 $cm^2\ C^{-1}$ (λ = 602 nm), achieved at −1.0 and −1.5 V for the PEDOT–PANI and PEDOT–PB devices have been correlated to the particularly low magnitude of charge transfer resistance and high polarization capacitance operative at the PEDOT–ionic liquid based electrolyte interface at these dc potentials, thus allowing facile ion-transport and consequently resulting in enhanced absorption modulation. Moderately fast switching kinetics and the ability of these devices to sustain about 2500 cycles of clear-to-dark and dark-to-clear without incurring major losses in the optical contrast, along with the ease of construction of these cells in terms of high scalability and reproducibility of the synthetic procedure for fabrication of the electrochromic films and the ionic liquid based gel electrolyte film, are indicators of the promise these devices hold for practical applications like electrochromic windows and displays.

1. Introduction

Conducting polymer based electrochromic devices have generated significant attention owing to their reversible conversion between two or more redox states, small response times, high contrast ratios, ease of preparation by chemical or electrochemical routes and high scalability of the electrode films.[1,2] Poly(3,4-ethylenedioxythiophene) or PEDOT in particular has aroused much interest as a cathodic electrochrome due to its rapid and reversible switching between deep-blue and pale-blue hues, the large electronic conductivity of its p-type state, high transmissivity for visible radiation in its oxidized form and the high stability of its doped state.[3–6] Furthermore, the high insolubility of the polymer also aids in inhibiting its dissolution in the electrolyte during electrochemical cycling. Among anodic coloring electrodes, polyaniline (PANI)[7] and Prussian blue (PB)[8,9] independently, and in the form of a bilayered assembly,[10] have been extensively utilized owing to their diverse colors and their ability to color and bleach simultaneously with the primary electrode. The complementary coloring layer, PANI, colors green and then turns blue depending on the level of oxidation and switches to transparent yellow in the reduced state. Prussian blue is blue in the oxidized state and colorless in the reduced state. Though electrochromism in these films has been studied exhaustively in the past,[11–13] the electrochemistry, optical properties and switching rates of devices based on these films are not yet fully understood. Similarly, electrolytes based on ionic liquids are in-vogue for the entire spectrum of solid-state electrochemical cells due to the several advantages of ionic liquids over traditional salts.[14,15] For instance, the use of a hydrophobic ionic liquid makes the electrolyte less susceptible to moisture-uptake unlike the traditional hygroscopic lithium- or proton-conducting electrolytes, wherein the salts promptly adsorb moisture when handled in non-inert conditions.[16,17] Furthermore, the use of ionic liquid electrolytes for generation of electroactivity in the polymer is known to impart a long-term cycling-stability to polymer films.[16–18] The pyrrolidinium ion, being organic, is not as easily solvated as Li^+ or H^+ or Na^+ and, therefore, higher ionic mobilities are achieved.[19] As the pyrrolidinium ion is larger and less-polarizing than alkali metal ions, Coulombic interactions are minimal and therefore the free ion concentration will be high. Faster switching times

National Physical Laboratory, Dr K.S. Krishnan Road, New Delhi, 110012, India. E-mail: m_deepa@mail.nplindia.ernet.in
† Electronic supplementary information (ESI) available: Additional experimental details. See DOI: 10.1039/b900091g

and amplified optical modulation are therefore expected. But reports on fabrication of ionic-liquid-based distensible, self-supporting gel–polymer electrolyte films are rare. Here we report the electro-syntheses of nanostructured electrochromic films of PEDOT, PANI and PB and fabrication of PEDOT–PANI and PEDOT–PB devices containing a gel electrolyte film of the ionic liquid: 1-butyl-1-methyl pyrrolidinium bis(trifluoromethylsulfonyl)imide (BMePyTfI). To date, rather narrow views of device performance have been reported and, therefore, this report attempts to provide new insights pertaining to the electrochemistry of devices during coloration and bleaching. Herein, the electroactivity of the primary and counter electrodes has been followed by cyclic voltammetry and impedance spectroscopy, whereby the dependence of the various redox processes on applied potential has been studied and correlated to the electrochromic coloration efficiency which, in turn, is governed by the intercalated charge density.

PEDOT films have been grown from an economical route involving an aqueous formulation of the monomer EDOT with an anionic surfactant.[20] The surfactant in the electropolymerization bath in addition to supplying counterions also controls the nanostructures of the resulting polymer deposit: grain size, distribution and porosity.[21–23] So that a facile exchange of ions is effected during the electrochemical measurements of the PEDOT–PANI device encompassing the imide based gel electrolyte, a small quantity of lithium imide was also added to the electropolymerization bath of PANI film as this enabled the doping of the radical cation by both chloride and imide ions. Electrochromism in polyaniline has often been restricted to narrow voltage ranges of −0.4 to +0.6 V for the leucoemeraldine base (LB) ↔ emeraldine salt (ES) ↔ pernigraniline (PG) transitions[24] to a still narrower range of −0.5 to +0.3 V.[7] Although a cycling life of a million cycles has been reported for PANI within a potential domain of −0.2 to +0.6 V[25] in an aqueous liquid electrolyte, the presence of ample proportions of volatile solvents in the electrolyte (even if it is a non-aqueous one) severely limits the utility of this system for any practical or commercial application. Consequently, the use of gel–polymer electrolyte films based on an ionic liquid overcomes this limitation thus offering the prospect of using the same even in commercial devices. The purpose of introducing a small proportion of a co-solvent that is perfectly miscible with the ionic liquid, namely dimethyl sulfoxide (DMSO), to the electrolyte here is for enabling gel formation with the polymer poly(vinyl alcohol) or PVA. We found that the conductivity change ongoing from the neat ionic liquid to the polymer–gel electrolyte film, was probably not much because the pure ionic liquid will have a high content of ion-pairs and upon dilution with DMSO, ion-pair dissociation and faster ionic mobility (due to viscosity a decrease) act to enhance conductivity. Thus, small quantities of ionic liquid suffice to produce electrolytes with high conductivities. The gel films thus formed are not only highly conducting but are also highly cost-effective. As the solid polymer electrolyte remains transparent and homogeneous with no visible phase separation or particulate formation and since no inert conditions (like a glove box) were employed to prepare or store the electrolyte, it was evident that PVA produces electrolytes with good dimensional stability. The methodology proposed is not restricted to the electrolyte film synthesized herein, but can be adapted to other ionic liquids and conventional salts as well.

2. Experimental

2.1 Synthesis of PEDOT, PANI and PB films

A 0.07 M 3,4-ethylenedioxythiophene (EDOT, Aldrich), 0.25 M sodium dioctyl sulfosuccinate solution in deionized water was used for electropolymerization under constant dc potential of +1.2 V for 240 s.[20] An inorganic transparent electrode (SnO_2 : F coated glass) was used as working electrode, a platinum sheet (Aldrich) as counter electrode and a Ag/AgCl/KCl electrode was used as reference. A 0.4 M solution of $C_6H_5NH_2$ (aniline, Merck), double distilled at ~100 °C at ambient pressure, 0.2 N HCl and 0.05 M $LiN(CF_3SO_2)_2$ (lithium bis(trifluoromethanesulfonyl)imide, 3 M) in deionized water was used for potentiodynamic electropolymerization of aniline in the voltage range of −0.2 to +1.1 V for ten cycles in a three-electrode electrochemical cell, similar to the above-described one. Prussian blue films were grown from a solution of 10 mM $K_3[Fe(CN)_6]$ (potassium hexacyanoferrate, Merck) and 10 mM $FeCl_3$ (ferric chloride, Qualigens) in 0.01 N HCl in a two electrode cell by galvanostatic electrodeposition by applying a fixed current density of 10 μA cm^{-2} to a SnO_2 : F coated glass substrate for eight minutes. The counter electrode was also a SnO_2 : F coated glass substrate of the same dimensions. All the as-obtained PEDOT, PANI and PB films were rinsed in deionized water, dried and stored in air. PEDOT and PANI films were grown using a Gamry Reference 600 and PB films were deposited with a Keithley 2400 current source.

2.2 Synthesis of electrolyte film, device fabrication and characterization methods

Polyvinyl alcohol or PVA was dried for 24 h at 80 °C prior to use. PVA (6 wt%) was dissolved in a 0.2 M BMePyTfI (1-butyl-1-methylpyrrolidiniumbis(trifluoromethylsulfonyl)imide, Merck) solution in dimethyl sulfoxide (DMSO, Merck) at 70 °C with rigorous stirring for 6 h. The resulting transparent viscous solution was poured into Petri dishes and stored at room temperature for five days for gelation and self-supporting film formation. The film thickness was approximately 340 μm. The electrolyte film was cut to size of the active electrode area using a scalpel blade and inserted between the PEDOT and PANI/PB layers, as shown in Fig. 1. As the gel film was free standing (inset of Fig. 1b), no additional spacer was required to hold the electrolyte in place. The neat electrolyte film showed a transmittance of ~70–80% in the visible region (recorded with respect to air, Fig. 1b). The linear sweep voltammogram recorded for the electrolyte film sandwiched between two SnO_2 : F coated glass electrodes showed it to be electrochemically stable between −3.0 to +2.5 V (Fig. 1c). Room temperature conductivity of the neat ionic liquid (1.25×10^{-3} S cm^{-1}) was measured on a Metrohm 712 dc conductometer and the conductivity of the polymer electrolyte film (5.3×10^{-3} S cm^{-1}) was measured by ac impedance spectroscopy wherein an electrolyte film was sandwiched

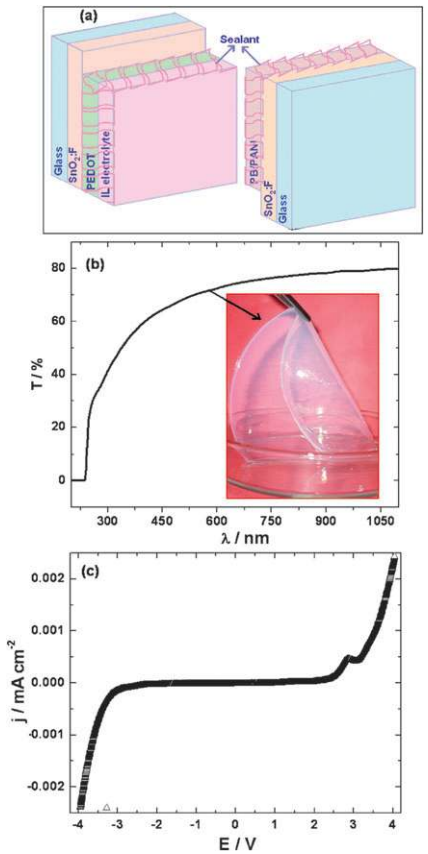

Fig. 1 (a) Schematic of the construction of the multi-layered devices; (b) transmittance of the neat polymer electrolyte film (photograph shown in the inset) in the 200–1100 nm wavelength region; and (c) linear sweep voltammogram of the neat electrolyte film between two SnO_2 : F electrodes recorded from −3.5 to +3.5 V.

between two platinum electrodes. These properties rendered it suitable for electrochromic device application. The whole device structure was held together with binder clips and the sealant (cyanoacrylate adhesive, Permabond, Aldrich) was applied by running the nozzle along the four sides of the device. The sealant cured within a few hours at ambient temperature. After removal of binder clips, the devices were ready for use. The approximate geometric active area of the devices was 4 cm × 3 cm. SEM images of the films were acquired on a LEO 440 microscope. Absorbance spectra of the devices were recorded *in situ* in the 300–1100 nm wavelength range with respect to air in the reference beam in a Perkin-Elmer Lambda 25 spectrophotometer. The films were colored and bleached by application of different DC potentials for 30 s, for saturation of the optical state. Switching time characteristics between the colored and bleached states for the devices were recorded by multiple step chronoamperometry with an indigenously developed microprocessor-controlled setup. The devices were illuminated with an He–Ne laser beam of λ = 632.8 nm and a silicon photodiode was used to sense the light intensity transmitted through the device. The transmittance/current *versus* time transients were recorded at frequencies of 0.011 and 0.012 Hz, when a square wave potential of ±1.0/±2.0 V was applied to the devices. All cyclic voltammetry and electrochemical impedance experiments were performed on a Gamry Reference 600.

3. Results and discussion

3.1 Cyclic voltammetry

In order to obtain complete information about the redox processes of the anodic and cathodic layers, cyclic voltammograms were recorded for the two devices, wherein PEDOT and PANI/PB were alternately employed as working electrodes (Fig. 2). The oxidation of PANI usually occurs in two steps between +0.1 and +0.8 V in an aqueous acidic electrolyte for the leucoemeraldine base to emeraldine salt and from emeraldine salt to pernigraniline transition,[26] but here, only a small peak is seen at ~ +0.7 V in the curve recorded at 100 mV s^{-1}, when PANI was used as a working electrode (Fig. 2b). This is attributed to kinetic effect, the slow exchange of imide anions of the electrolyte with the imide and chloride ions present in the polymer film, which in turn is effected by compact coil structures in polyaniline, as can be seen from the micrograph in Fig. 3a and b. The position of this oxidation wave was found to vary a little with scan rate. Contrary to the reports in the past where the electrochemistry of PANI has been investigated in conventional alkali metal ion electrolytes,[7,25] very rapid deterioration of the film was observed *via* irreversible side reactions, the proof of which was observed by the authors in the form of oxidation and reduction peaks at +0.4 and +0.75 V thus rendering their films grayish-black, here, no such discoloration was observed. The oxidative degradation of PANI is caused by the hydrolysis of imine bonds in the fully oxidized pernigraniline form of PANI.[27] To avoid these irreversible degradation reactions, films are usually electrochemically probed between −0.2 V and +0.6.[7,25] On the other hand, here the PANI film's fibrillar morphology and the ionic liquid based electrolyte are largely responsible for the reversible oxidation–reduction yellow-to-green process of PANI, free of any degradative reactions between +1 V and −1 V. In the reduction cycle, corresponding to the de-doping of imide ions, a broad plateau-like response is observed at all scan rates (Fig. 2b), with a faint hint of a peak at −0.5 V only at 75 mV s^{-1}. The broad cathodic wave shows no distinct redox peak, as the rate of pyrrolidinium ion elimination in the anodic process is greater than that of the cation intercalation reaction in the cathodic process.[28] Judging by the basis of the shape of the voltammograms in both anodic and cathodic branches, the film appears to be highly capacitive, and this is also ratified from the magnitude of charge inserted during oxidation which is 23 mC cm^{-2}, and the same quanta of charge is extracted in the reverse cycle (at 100 mV s^{-1}), thus indicating good reversibility.

For the same device, when PEDOT was used as a working electrode (Fig. 2a), the oxidation peak at +0.2 V corresponding to the pale-blue-to-dark-blue transition is seen only at scan rates ≥ 30 mV s^{-1} and as in PANI, no distinctive peaks were observed in the reduction process at any scan rate. Activity on the reductive sweep is less-perceptible, probably due to chemical oxidation of reduced PEDOT by molecular oxygen trapped in the electrolyte. The inserted charge is 11 mC cm^{-2}

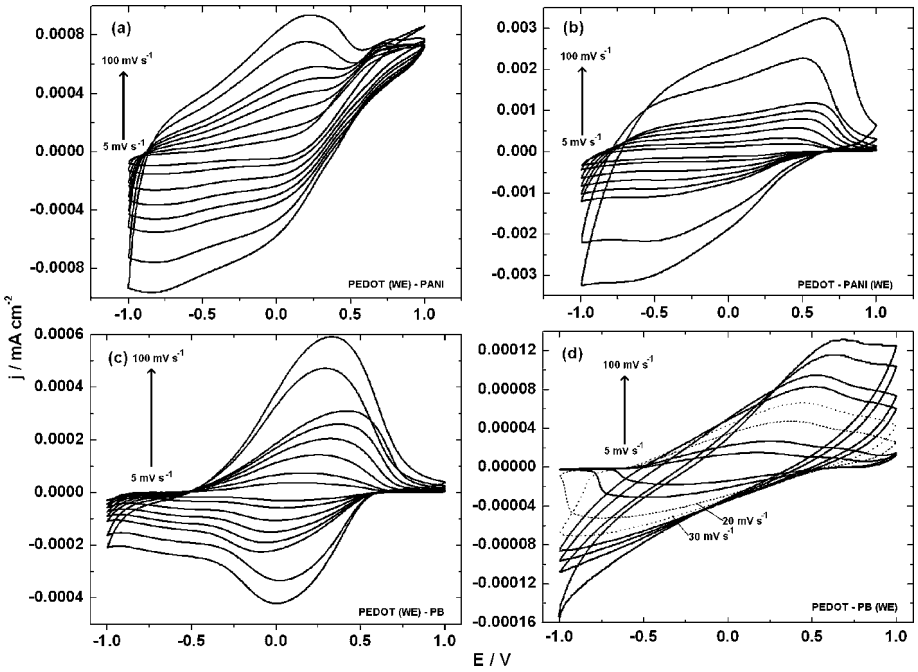

Fig. 2 Cyclic voltammograms of a PEDOT–PANI device with (a) PEDOT and (b) PANI films as working electrodes and a PEDOT–PB device with (c) PEDOT and (d) PB films as working electrodes within ±1.0 V at different scan rates of 5, 10, 20, 30, 40, 50, 75 and 100 mV s^{-1}.

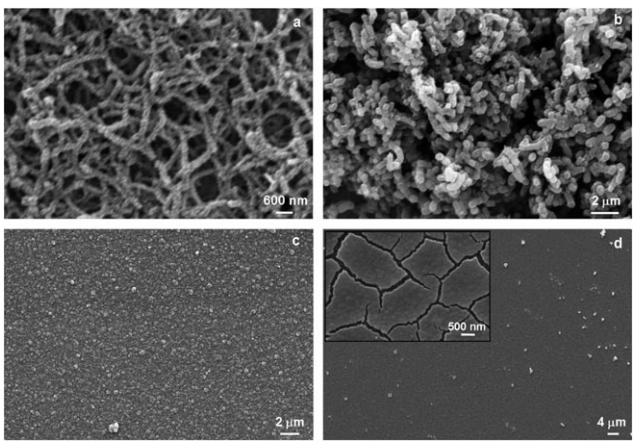

Fig. 3 SEM micrographs of the electroactive films: (a) elongated and (b) short fibers of PANI, (c) PEDOT and (d) PB used for fabricating the devices. Inset of (d) is the magnified view of PB film surface, illustrating the cracks formed on the uppermost layer of the film.

and the charge extracted is 7 mC cm^{-2} at 100 mV s^{-1}, which is much larger than charge capacities of 0.68 and 1.01 mC cm^{-2} achieved for PANI–PEDOT cells in ref. 24. For the individual PEDOT and PANI layers in ref. 24, the capacities were 0.49 and 4.6 mC cm^{-2}, and PEDOT was deduced to be the rate-limiting moiety for the device. Here too, the polyaniline film, as proven by charge capacities, is more capacitive than the primary electrochrome, PEDOT. For the PEDOT–PB device, when PEDOT was employed as working electrode, at a sweep rate of 100 mV s^{-1} (Fig. 2c), the cathodic–anodic peak separation is quite small (0.3 V). It is an unusual occurrence, indicating that both redox processes occur within a narrow potential window of +0.30 and ~0.0 V. Upon increasing scan rate, the oxidation peak shifts from +0.4 V (at 50 mV s^{-1}) to +0.3 V (at 75 mV s^{-1}) and reduction peak from –0.01 (at 50 mV s^{-1}) to +0.09 V (75 mV s^{-1}). This abrupt shift of oxidation potential to lower values and reduction potential to higher values shows that cation diffusion is hindered and anion diffusion is relatively easier at high scan rates.[29]

With PB as the working electrode (Fig. 2d), the oxidation peak is seen at +0.65 V (s = 100 mV s^{-1}), and this systematically shifted to lower potentials, to +0.20 V at the lowest scan rate of 5 mV s^{-1}. The reduction peak was seen only in the scan rate range of 5–30 mV s^{-1} as at higher sweep rates, the profile was just a loop with no discernible redox peaks. At scan rates of 20 and 30 mV s^{-1}, the shape of the curve changed markedly, the film showed pronounced capacitive charging. At 20 mV s^{-1}, the inserted/extracted charge is ~2 mC cm^{-2}, whereas at 100 mV s^{-1}, the film is no longer capacitive, the inserted/extracted charge is ~0.6 mC cm^{-2}. At 100 mV s^{-1}, the intercalated/deintercalated charge is slightly higher for the primary electrode PEDOT; it is approximately 1 mC cm^{-2}. While the CV profiles of PEDOT and PANI do not differ much, the curves for PEDOT and PB are distinctly different, indicating that the electrochemical response of the two conjugated polymers is similar, but differs from that of the inorganic mixed valence complex. All the three electrodes: PEDOT, PANI and PB films; exhibit a linear increase in peak current with the square-root of scan rate, confirming that the films allow a semi-infinite diffusion of ions. This straight-line behavior of the plots for variation of peak currents as a function of square root of sweep rate (denoted by "s") of the PEDOT–PANI device (Fig. 4) was found to deviate from this trend at high scan rates of 75 and 100 mV s^{-1}, in both anodic and cathodic scans, when PANI was used as a working electrode, indicating the presence of surface confined redox species.[24]

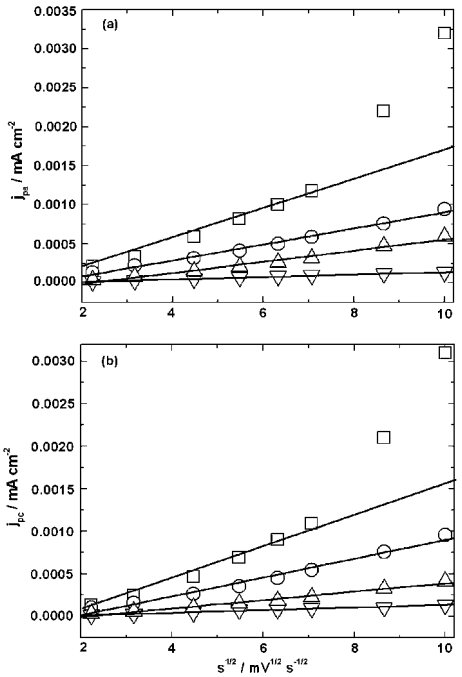

Fig. 4 Plots of (a) anodic and (b) cathodic peak current *versus* square root of scan rate for PEDOT (○) and PANI (□) as working electrodes in PEDOT–PANI device, PEDOT (△) and PB (▽) as working electrodes in PEDOT–PB device. Solid lines represent linear fits.

3.2 Spectroelectrochemistry

The absorbance of the as-fabricated PEDOT–PANI and PEDOT–PB devices recorded under different oxidation and reduction potentials are shown in Fig. 5a and b. The absorption peak at 445 nm in the as-fabricated PEDOT–PANI device (Fig. 5a) confirms that the as-deposited PANI film is in the green emeraldine-salt form: the widely-known conducting form. This peak originates from radical cations, more specifically due to the polaron-π* transitions,[30] and shows a maximum value at $E = -0.5/-0.75$ V, and is retained in the coloration efficiency plot as well. High doping levels in polyaniline are usually responsible for this peak and here, the compact coil conformation of PANI, realized in the form of fiber like shapes (Fig. 3a and b), ensure a high dopant uptake during electrolytic oxidation. Here, the blue pernigraniline form is achieved at $E \geq -1.25$ V, and as expected, the 445 nm absorption is lost at these potentials. Broad absorption in the NIR region (~750 to 1000 nm) in the as-fabricated device includes mixed contributions from the bipolaronic states of PEDOT[31] and the π-polaron transitions in oxidized PANI.[30] The intense absorption in the 590–600 nm range, is due to π–π* transitions of PEDOT,[31] with a maximum at $E = -1.5$ V and its intensity declines at higher negative potentials and the same holds true for the PEDOT–PB device. It is possible that no-more electrochemically addressable sites are left in the active electrode film (be it PEDOT or PANI or PB) for the electrolyte ions to have access to, and therefore the additional inserted/extracted charge produced at high reducing voltages of −1.75 and −2.0 V (applied to PEDOT as working electrode, PB/PANI are counter electrodes) can trigger degradative effects and, as a consequence, absorption is quenched at these high potentials.

The as-fabricated PEDOT–PB device shows a broad absorption peak at ~900 nm due to the presence of bipolarons, indicative of the oxidized form of PEDOT (Fig. 5b). The same peak is also observed when the PEDOT electrode was subjected to oxidation potentials of +0.5 and +1.0 V. Upon application of −1.0 V, the intensity of this peak is reduced at the expense of another new peak due to π–π* transitions at ~590 nm. The intensity of this peak is significantly enhanced at −1.5 V and the peak due to bipolaronic states ceases to exist, suggestive of the formation of the fully reduced state of PEDOT. For the PEDOT–PB device, in the as-fabricated state and under low negative potentials of −0.5 and −0.75 V, PEDOT and PB exist in partially reduced and partially oxidized states, respectively and at positive potentials of +0.5 and +1.0 V, fully oxidized and fully reduced forms of PEDOT and PB exist; the broad absorption peak in the 750 to 1100 nm range is due to the bipolaronic states of PEDOT. Surprisingly, the expected absorption peak at 790 nm due to Prussian blue,[32] is not seen under any of the reduction dc conditionings applied to PEDOT.

The wavelength dependence of coloration efficiency (η), which is defined as the change in the optical density (ΔOD) for the charge (q) consumed per unit electrode area (A), is also shown in Fig. 5c and d.

$$\text{CE } (\eta) = \Delta\text{OD } (\lambda)/(q/A) = \log (T_b/T_c)/(q/A) \qquad (1)$$

T_b and T_c are the transmittances of the device in the bleached and colored states respectively. Gaupp *et al.*[33] proposed that CE values calculated for ΔT ranging from 80 to 100% of the maximum optical contrast for PEDOT and its analogues enable quantitative comparisons. In a similar manner, we determined coloring efficiencies for the two devices at different potentials of −0.5, −0.75, −1.0, −1.25, −1.5, −1.75 and −2.0 V, with the reference voltage being fixed at +1.0 V. These reduction potentials (with respect to PEDOT) corresponded to ~42, 59, 87, 89, 100, 98 and 96% (for the PEDOT–PANI device, Fig. 5c) and to ~13, 20, 44, 50, 100, 92 and 84% (for the PEDOT–PB device, Fig. 5d) of the full switch at λ_{max} that lies in the range of 580–600 nm. The highest coloration efficiency maximum (η_{max}) of 274 cm^2 C^{-1} (λ = 602 nm) of the PEDOT–PB device achieved under $E = -1.5$ V is slightly lower than η_{max} of 281 cm^2 C^{-1} (λ = 583 nm) obtained for the PEDOT–PANI device under an even lower E of −1.0 V. This η_{max} corresponds to 100% (or maximum contrast) for the PEDOT–PB device whereas for the PEDOT–PANI device, η_{max} is achieved for 87% of the total switch, suggesting that charge utilization is more effectual for inducing coloration in this device, than in the PEDOT–PB device. For the PEDOT–PB device, η_{max} reduces to 236 cm^2 C^{-1} (λ = 602 nm) at $E = -1.75$ V which corresponded to 92% of the maximum contrast and further decreases to 206 cm^2 C^{-1} (λ = 602 nm) at −2.0 V (for 84% of the full switch); the latter value being lower than η_{max} achieved at −1.0 V (231 cm^2 C^{-1} at 590 nm), thus indicating that large charge densities are not necessary for the attainment of high visible coloration efficiency maxima.

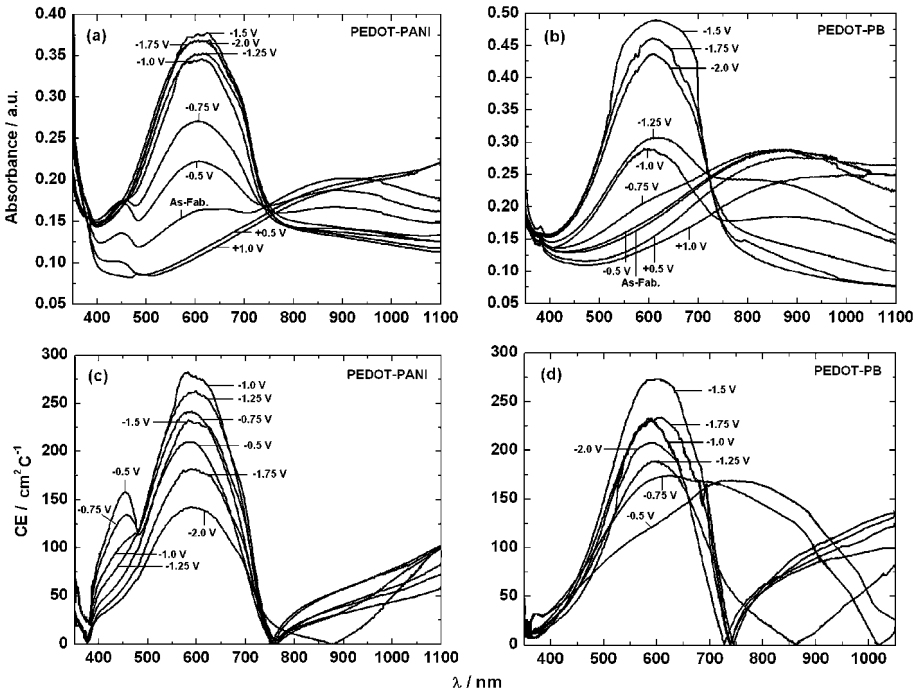

Fig. 5 *In situ* absorbance spectra of (a) a PEDOT–PANI and (b) a PEDOT–PB device, recorded under different oxidation and reduction dc potentials applied for 30 s each and in their as-fabricated states. Coloration efficiency plots of (c) a PEDOT–PANI and (d) a PEDOT–PB device; the optical states under +1.0 V in (a) and (b) have been taken as reference for the two devices, respectively.

The PEDOT–PANI device (Fig. 5c) shows two distinct η_{max}, the first one in the 450–500 nm range and the second in the 580–600 nm range; the highest values for these two maxima are not however acquired at the same potential. The highest η_{max} of 157 cm^2 C^{-1} at 455 nm is achieved under −0.5 V and the corresponding η_{max} at 589 nm is 210 cm^2 C^{-1}. At the higher photopic wavelength of 583 nm, the highest η_{max} is 281 cm^2 C^{-1}, shown by the PEDOT–PANI device at −1.0 V corresponding to 87% of the full switch, and this clearly surpasses the CE shown by the same device at this wavelength at −0.5 V. Even at the lowest reduction potential of −0.5 V, corresponding to 42% of the total switch, that a CE_{max} of 210 cm^2 s^{-1} could be achieved, again confirms that the charge intercalated allows an optimum consumption of the redox active sites on the functional electrode. Previously, coloration efficiencies of 285 and 338 cm^2 C^{-1} for PEDOT–PANI and PEDOT–PB devices were observed at 570 and 590 nm wherein an $LiClO_4$ based electrolyte was used.[7,8] In another report, a coloration efficiency of 302 cm^2 C^{-1} (λ = 560 nm) was realized by Fabretto *et al.*[34] for a PEDOT–PANI device and this corresponded to 95% of full switch. In yet another report,[33] a composite CE of 206 cm^2 C^{-1} was observed for PEDOT at λ_{max} of 585 nm, for 80% of the maximum contrast. Our values agree reasonably well with reported values.

It is noteworthy that the highest coloration efficiency maxima are achieved under −1.5 V and −1.0 V for the PEDOT–PB and PEDOT–PANI devices respectively and not at −2.0 V, which is the highest applied potential in this study. This demonstrates that a lower value of intercalated/deintercalated charge density is adequate enough to bring about a larger optical contrast and this is most advantageous for maximizing the cycling life of the device. This is also corroborated by Argun *et al.*[1] and Rauh *et al.*,[35] as authors also observed that at high doping levels, as percent transmittance saturates, coloration efficiency drops owing to charge consuming side reactions. Further discussion on coloration efficiency of PEDOT–PB and PEDOT–PANI devices can be found in the ESI.†

3.3 Electrochemical impedance spectroscopy (EIS)

On superimposition of a sinusoidal ac voltage of 5 mV over a fixed dc potential of different magnitudes, in both devices, the ensuing EIS plots comprise one or two semi-circles with or without an inclined straight line portion. The impedance of the two electroactive electrodes that constitute the devices has been recorded in the following manner: the impedance of the cell (PEDOT–PANI) was measured by using PEDOT as the working electrode and a dc potential of −0.5 V was applied to it and compared with the response of the same cell, when PANI was used as a working electrode and a dc potential of +0.5 V was applied to it. A complete picture of the redox phenomena at both electrodes is expected to emerge from such a comparison, for when a certain magnitude of dc potential is applied to the working electrode (WE) (be it PEDOT/PB/PANI), the counter electrode (it will be PANI/PB if the WE is PEDOT, and it will be PEDOT if the WE is PANI/PB) is assumed to be subjected to a dc potential of the same magnitude but reverse polarity. Such comparative experiments were therefore performed for both devices at dc potentials of 0, 0.5 and 1.0 V. A comparison of the experimental and fitted (calculated) impedance spectra of the devices is shown in Fig. 6 and 7 and a full tabulation of the parameters is provided in Tables 1 and 2. The equivalent circuit displayed in Fig. 8 was

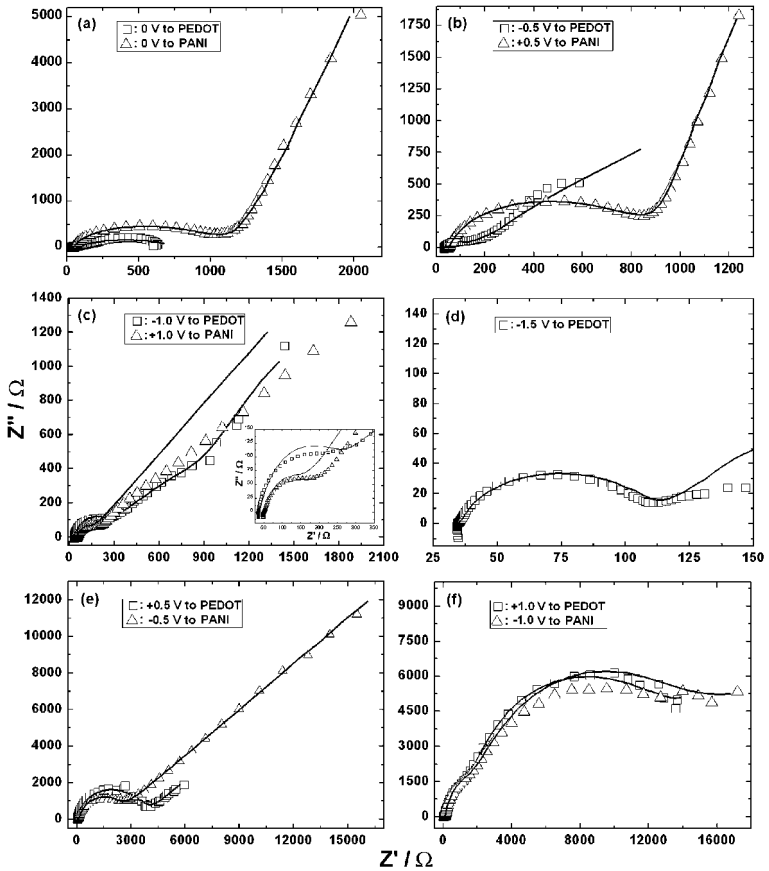

Fig. 6 Nyqvist plots of PEDOT–PANI device recorded under an ac amplitude of 5 mV, at different DC potentials: (a) as-fabricated state, (b), (c) and (d): device in colored state and (e) and (f): device in bleached state. Symbols (□, ○) represent the experimental data and the solid lines (—) are obtained by fitting the experimental data in the model shown in Fig. 8.

found to give good fits almost over the entire frequency range of 1 MHz to 1 mHz under consideration. The start of the first semicircle is ascribed to the uncompensated bulk resistance of the ionic liquid based solid polymer electrolyte which lies in the range of 30–50 Ω; its value was found to be largely independent of the applied dc bias. Resistance due to contacts and counter electrode also contribute to R_S.[36] The R_S here is significantly lower than that reported for a PEDOT symmetrical device which is 386 Ω.[37] For a Pt/PEDOT/0.1 M KCl system, R_S was 122 Ω.[38]

Polarization resistance (R_P) and capacitance (C_P) due to separation and accumulation of charges at the respective electrodes produce the first semicircle which is followed by the second semicircle which involves a parallel combination of interfacial resistance due to charge transfer (R_{CT}) and the corresponding electrical double layer capacitance (C_{dl}). C_{dl} has been expressed in terms of CPE1 as it takes into account: (i) the depression in the second semicircle; and (ii) the deviation from the ideal 45° slant of the classical finite length Warburg diffusion line. CPE2 corresponds to the phase offered by the counter electrode to the total impedance, which can be visualized as an infinite resistance connected in parallel with it. The redox propagation in the colored and bleached states of the two devices has been illustrated in Fig. 9. In the no dc bias scenario (Fig. 6a), the polarization and charge transfer resistances are higher and lower, respectively for PANI (R_P = 700 Ω and R_{CT} = 218 Ω) than that of PEDOT (R_P = 27 Ω and R_{CT} = 714 Ω) and the same trend is retained when PEDOT is reduced by −0.5 V and PANI oxidized by +0.5 V (Fig. 6b). The polarization resistance is much lower for PEDOT (63 Ω) than that of PANI (528 Ω) whereas the reverse is true for R_{CT}, it is 1249 Ω for PEDOT and 270 Ω for PANI (Fig. 6b). This is natural, as the greater the available driving force, the greater would be the accumulation of cations and anions at the cathode and anode. It should be noted that upon removal of anions from the film during reduction of PEDOT, it acquires the neutral non-conducting neutral state, whereas PANI upon anion incorporation becomes conducting, so a greater R_{CT} for PEDOT is explained at −0.5 V.

At −1.0 V to PEDOT, R_{CT} is much lower for PEDOT (1.0 Ω) than R_{CT} of PANI (41 Ω) (Fig. 6c). On applying +1.0 V to PANI, the conversion of the green emeraldine salt to the blue pernigraniline form occurs. It is well-known from literature that the electronic conductivity of the ES form is much greater than that of the PG state and this should act to lower the resistance to charge transfer and the same occurs. R_{CT} for both electrodes are also lower than their values at −0.5 V to PEDOT and +0.5 V to PANI. It is under −1.0 V, η_{max} was obtained for the PEDOT–PANI device. At this conditioning, as can be judged from the figure, the overall Z' *versus* Z'' response also match exceedingly well for two electrodes. This indicates that the reaction in the electrochromic

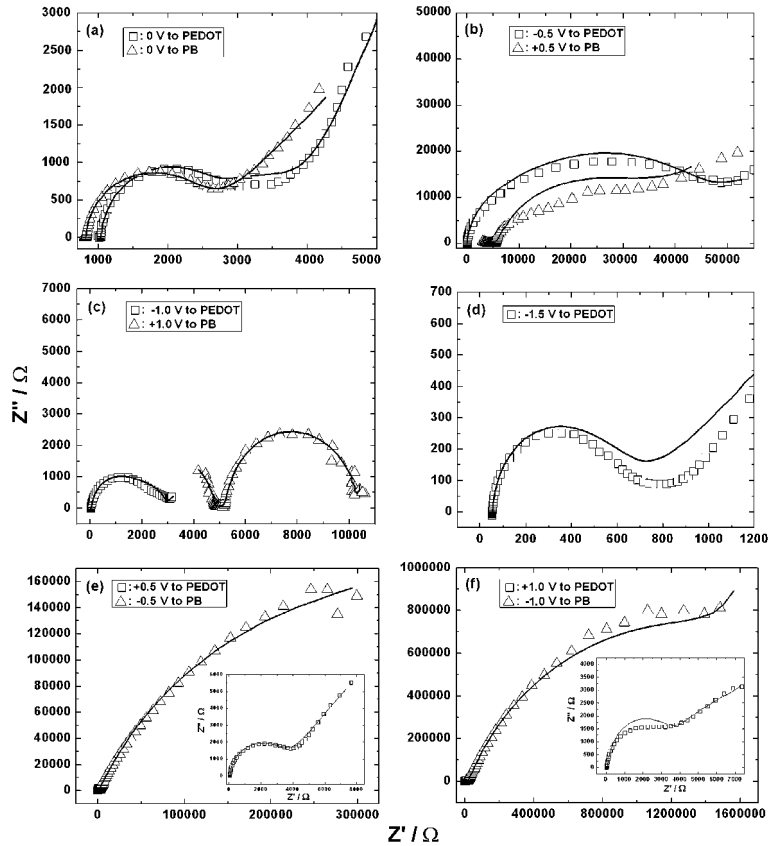

Fig. 7 Nyqvist plots of PEDOT–PB device recorded under an ac amplitude of 5 mV, at different dc potentials, (a): as-fabricated state, (b), (c) and (d): device in colored state and (e) and (f): device in bleached state. Symbols (□, ○) represent the experimental data and the solid lines (—) are obtained by fitting the experimental data in the model shown in Fig. 8.

Table 1 Electrochemical impedance spectroscopy results for PEDOT and PANI as working electrodes in PEDOT–PANI device, obtained by fitting the experimental data in the model shown in Fig. 8

Applied E/V		R_P/Ω		R_{CT}/Ω		C_P/F		Y_0/S (s)$^{1/2}$	
PEDOT	PANI	PEDOT	PANI	PEDOT	PANI	PEDOT	PANI	PEDOT	PANI
−0.5	+0.5	63	528	1249	270	148.6×10^{-6}	5.0×10^{-6}	4.45	7.3×10^{-3}
−1.0	+1.0	150.4	66	1	41	233×10^{-6}	77.3×10^{-6}	2.8×10^{-3}	6.1×10^{-1}
−1.5	—	1	—	60	—	1.3	—	10	—
0	0	27	700	714	218	84.6×10^{-6}	88.3×10^{-6}	599	5.1×10^{-3}
+0.5	−0.5	1544	1800	2130	2	73.7×10^{-6}	209.5×10^{-6}	2.8×10^{-3}	5.2×10^{-3}
+1.0	−1.0	1160	1379	9740	12 330	77.0×10^{-6}	286.9×10^{-6}	1.2×10^{-3}	0.7×10^{-3}

Table 2 Electrochemical impedance spectroscopy results for PEDOT and PB as working electrodes in PEDOT–PB device, obtained by fitting the experimental data in the model shown in Fig. 8

Applied E/V		R_P/Ω		R_{CT}/Ω		C_P/F		Y_0/S (s)$^{1/2}$	
PEDOT	PB	PEDOT	PB	PEDOT	PB	PEDOT	PB	PEDOT	PB
−0.5	+0.5	9820	705	34 100	3160	1.5×10^{-4}	5.5×10^{-10}	6.8×10^{-4}	4.8×10^{-4}
−1.0	+1.0	1410	3080	1550	4760	9.2×10^{-5}	2.4×10^{-11}	7.7×10^{-2}	6.1×10^{-1}
−1.5	—	384	—	0.4	—	7.8×10^{-5}	—	1.6×10^{-2}	—
0	0	1530	1195	972	745	1.2×10^{-4}	1.5×10^{-4}	2.6×10^{-2}	2.4×10^{-3}
+0.5	−0.5	2690	198	459	4.4×10^{5}	3.2×10^{-4}	1.8×10^{-10}	1.2×10^{-3}	2.5×10^{-5}
+1.0	−1.0	2530	3300	7200	1.7×10^{6}	2.9×10^{-4}	3.9×10^{-11}	7.3×10^{-3}	4.0×10^{-6}

working electrode is well balanced by the reaction in the coloring counter electrode and the undesired reactions such as production of chemical species which either degrade the functional electrodes or simply consume charge without inducing optical change are at a minimum, thus manifesting in a large CE for this device. The diffusion phenomena in the low frequency region are also comparable for both electrodes when −1.0 V is applied to PEDOT and +1.0 V is applied to PANI

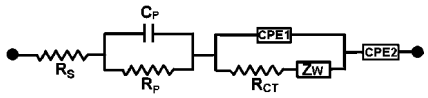

Fig. 8 Randles equivalent circuit for the PEDOT–PANI and PEDOT–PB devices.

(Fig. 6c). As the device goes from the state with PEDOT in the partially reduced state (−0.5 V), to a state with fully reduced PEDOT (−1.0 V), the impedance for ionic movement through the bulk of the film or diffusion at high potentials goes from capacitive to resistive, for either removal of anions from PEDOT or migration of counterions in PANI. This is evident in the form of the pronounced deviation of the Warburg line from 45° more towards the abscissa than towards the ordinate. It is also reflected in the decrease in the component α: from 0.49 (PEDOT, −0.5 V) to 0.091 (PEDOT, −1.0V) of CPE1 (which is associated with C_{dl}). The polarization capacitance is generally of the order of a few tens to hundreds of microfarads for both electrodes, except for an aberration or two (Fig. 6). The polarization capacitance is higher at both PEDOT (−0.5, −1.0 and −1.5 V) and PANI electrodes (+0.5 and +1.0 V) during coloration than during bleaching, indicating that anions are more easily available for doping of PANI and cations for charge neutralization after dedoping of PEDOT. Similarly the polarization resistances are also higher during oxidation of PEDOT (*i.e.* when PEDOT is kept at positive potentials irrespective of its use as a working or counter electrode); and the same is applicable to PANI in *vice-versa*.

It should be noted that anion removal will be accompanied by intercalation of charge compensating cations in PEDOT (Fig. 9a). The hindered diffusion of bulky cations (though less solvated, the substituted pyrrolidinium ion is a large molecule) and the large separation between polymer chains caused by large counterions (sulfosuccinate or imide) resist the propagation of charge through the bulk of the film. Upon application of −1.5 V to PEDOT (Fig. 6d), R_{CT} was 60 Ω and R_P is as low as 1 Ω, the latter indicating that a large bias assists charging of the primary electrode. When +0.5 V is applied to PEDOT (Fig. 6e), it reverts to the oxidized pale blue state, and at the anode, when PANI is subjected to −0.5 V, the yellow leucoemeraldine base form is formed. Fig. 9b shows the formation of the bleached states and redox behavior. While the polarization resistances of both electrodes are comparable at this juncture, R_{CT} for PEDOT (2130 Ω) is greater than that of PANI (2 Ω) by three orders of magnitude and this is reversed at the next potential. At −1.0 V to PANI and +1.0 V to PEDOT (Fig. 6f), R_{CT} increased at both ends of the device. For PANI, R_{CT} enhanced from 2 Ω to 12 330 Ω (by five orders of magnitude!). This enormous jump is probably due to the fact that −0.5 V suffices to bring about the complete reduction of PG to the LB form and therefore, at a higher negative potential of −1.0 V the film has a profoundly reduced affinity to undergo further dedoping. It therefore resists the removal of any further charge and R_{CT} increases by manifold times. For PEDOT subjected to +1.0 V (Fig. 6f), R_{CT} is 9740 Ω, lesser than that of its counter electrode undergoing reduction at the same E, but higher than its value at +0.5 V. For PEDOT, just like in case of PANI, beyond a certain level of doping, after the film is presumably saturated with imide ions, further uptake of ions will be inhibited and R_{CT} is expected to increase, and it does. Here, the Z' *versus* Z'' response is strikingly different for the two films in the Warburg region, the diffusional impedance has a much larger amplitude for PANI (in reduced state) than for PEDOT (in oxidized state) indicating that anion transport through the bulk of PEDOT is more facile than anion extraction from PANI. The overall impedance response is again comparable at +1.0 V to PEDOT and −1.0 V to PANI (Fig. 6f); the spread of this response is widest at this conditioning, which reiterates that under high potentials when the device is bleached, both the electrodes undergo similar electrochemistry, where resistance to charge transfer and ion transport through the bulk of the electrodes are greatly enhanced. The high R_P value

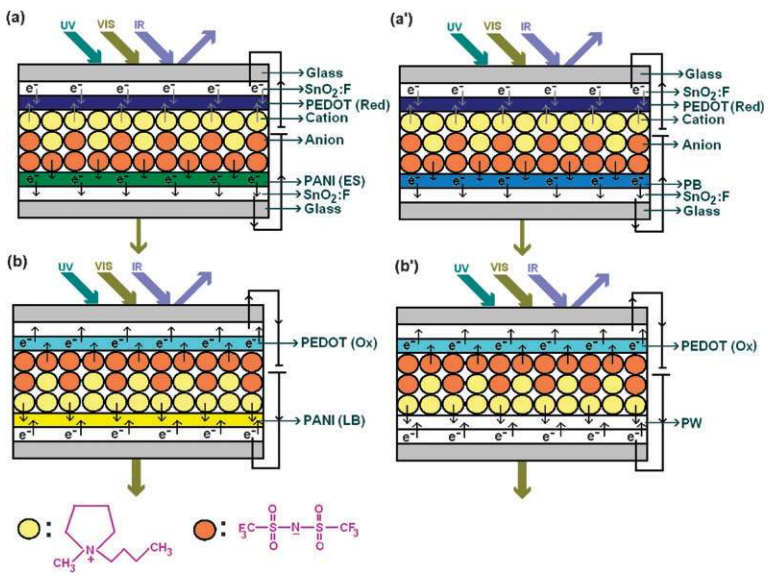

Fig. 9 Schematic of redox propagation in PEDOT–PANI and PEDOT–PB devices: In colored state: PEDOT in reduced state in (a) and (a′) and PANI (a) and PB (a′) in oxidized states and in bleached state: PEDOT in oxidized state in (b) and (b′) and PANI (b) and PB (b′) in reduced states.

for PEDOT (in oxidized state) is comparable to that reported for PEDOT in a symmetrical PEDOT device.[37]

In the PEDOT–PB device, charge transfer impedance during reduction of PEDOT (−0.5 V to PEDOT, Fig. 7b) is 34 100 Ω and R_{CT} at the counter electrode (+0.5 V to PB), wherein R_{CT} = 3160 Ω and the redox process can be seen in Fig. 9a′. The open ion-permeable morphology of PEDOT (Fig. 3c) allows facile anion insertion but its deintercalation is apparently not governed by microstructure. R_{CT} decreases to 1550 Ω at −1.0 V and further to as low as 0.4 Ω at −1.5 V (Fig. 7d). It should be recalled that the maximum CE was achieved under −1.5 V to PEDOT. The extremely low magnitude of R_{CT} clearly demonstrates the ease of charge transport across the PEDOT–IL polymer electrolyte interface, thus ensuing in a high CE. R_{CT} is low during oxidation (∼459 Ω at +0.5 V to PEDOT, Fig. 7e) and it increases to 7200 Ω on further oxidation (+1.0 V to PEDOT, Fig. 7f). At +1.0 V to PB, R_{CT} increases to 4760 Ω (Fig. 7c). R_P also follows a similar trend during reduction of PEDOT, as it decreases from 9820 to 384 Ω as E goes from −0.5 to −1.5 V and is slightly higher, but comparable, during oxidation of this electrode at +0.5 and +1.0 V (2690 and 2530 Ω, respectively, Fig. 7e and f). R_P decreases with applied E, during both the oxidation and reduction of PEDOT. At the counter electrode, PB, R_{CT} for reduction was found to be unusually large: 4.4×10^5 Ω (−0.5 V to PB, Fig. 7e) and 1.7×10^6 Ω (−1.0 V to PB, Fig. 7f). In PB, the reduction charge transfer resistances are much higher than the corresponding oxidative R_{CT} which shows that the bleaching of the film is obstructed. Fig. 9b' shows the redox configuration of the device in the bleached state. The film microstructure is known to affect bleaching rather than coloration. It is obvious that the dense morphology and the low porosity of the film inhibit charge transfer. While R_P, C_P and R_{CT} (of PB) be it oxidation or reduction, increase ongoing from ±0.5 V to ±1.0 V, for PEDOT, the trends are not so regular. PB therefore shows a driving-force-dependent enhancement of impedance while PEDOT does not show the same behavior. While capacitive polarization is in the range of 0.08 to 0.32 mF (over the entire potential range) for PEDOT, for PB, it is extremely low, of the order of 10^{-10}–10^{-11} F indicating that this electrode is not a good collector of either cations or anions.

In the Warburg region, the parameter Y_0 gives the measure of the ease of ion diffusion[39] as

$$Y_0 = 1/(2)^{1/2} \times \sigma \quad (2)$$

$$\sigma = 2RT/n^2 \times F^2 \times A \times (2D)^{1/2} \times C \quad (3)$$

where A is the area of the active electrode and C is the concentration of the ionic species in mol cm^{-3}. Since $Y_0 \propto (D)^{1/2}$, a high Y_0 implies rapid diffusion. Among all potentials, a high value of Y_0 is registered at −1.5 V to PEDOT (Y_0 = 10) for the PEDOT–PANI device. The diffusion coefficient is 4.4×10^{-7} cm^2 s^{-1}. A larger driving voltage allows faster expungement of counter ions from the bulk of the film during reduction, as D at –0.5 V to PEDOT is slightly lesser, it is 8.7×10^{-8} cm^2 s^{-1}. In the same device, during oxidation, D values are significantly reduced as $D = 0.35 \times 10^{-13}$ cm^2 s^{-1} (at +0.5 V to PEDOT) and $D = 0.6 \times 10^{-14}$ cm^2 s^{-1} (at +1.0 V to PEDOT), clearly suggestive of a rather restrained diffusion of dopant ions through the bulk of the electrode. The decrease in D with increasing E also shows that unlike during electrochemical dedoping of anions, a larger magnitude of external bias does not necessarily result in facile doping. Similarly, in the PEDOT–PB device, D increases from 0.2×10^{-14} cm^2 s^{-1} (at −0.5 V to PEDOT) to 0.1×10^{-11} cm^2 s^{-1} (at −1.5 V to PEDOT), whereas during oxidation, the D value is 0.7×10^{-14} cm^2 s^{-1} (under +0.5 V to PEDOT), which reduces to 0.4×10^{-15} cm^2 s^{-1} at +1.0 V to PEDOT. The D values, be it oxidized or reduced state, are much lower for the PEDOT–PB device in comparison to the PEDOT–PANI device and these are lower by a few orders of magnitude, at any given potential. The diffusion of ions in PB hindered by the presence of crisscross cracks, several microns in length, that are spread all across the film surface, and these are clearly visible in the inset of Fig. 3d.

3.4 Optical and electrical response at 632.8 nm

The transmittance/current–time transients recorded for the devices at 0.011 Hz at a monochromatic wavelength of 632.8 nm under square wave potentials of ±1 and ±2 V are shown in the ESI.† The total modulation of PEDOT–PANI was found to be about 62% of the total contrast attained by PEDOT–PB device. The coloration time is 2.5 s for a 90% decrease in transmittance of the PEDOT–PB device and this device takes 5.0 s for bleaching, to undergo a 90% increase in transmittance. These values are greater than our previously reported color–bleach times of 7.9 and 2.6 s for a 90% transmittance change in a PEDOT–PB device under ±1.5 V, where PEDOT was grown from a micellar solution of camphorsulfonate ions and a proton conducting electrolyte was used.[40] A typical photograph of a PEDOT–PB device in colored and bleached states is also shown in Fig. 10. Coloration and bleaching occur in 3.0 and 5.0 s, respectively for a 90% transmittance change in the PEDOT–PANI device. Coloration was observed to be faster than bleaching in both devices. Since leakage current has a larger magnitude during coloration than bleaching; this facilitates ion movement during coloration (see ESI, Fig. 1†). It was seen earlier that in the PEDOT–PB device, reduction of PEDOT is facile (at −1 V to PEDOT) as compared to PB's oxidation at the same bias, due to higher polarization capacitance, lower charge transfer impedance and fast ion diffusion in the high, intermediate and low frequency regimes respectively. These

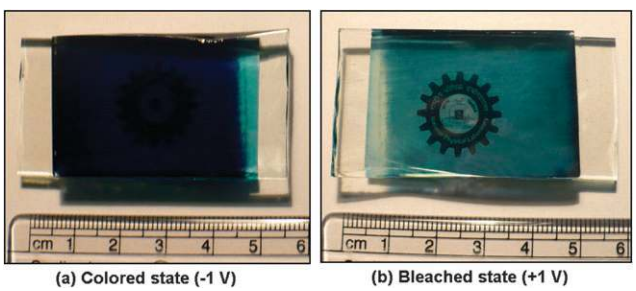

Fig. 10 Photographs of a PEDOT–PB device recorded in colored and bleached states.

factors also favor a faster coloring rate and therefore coloration times are short. The color–bleach response is however severely affected when the devices were subjected to multi-step chronoamperometry at a higher dc potential of ±2 V (see ESI, Fig. 2†). The total modulation of the PEDOT–PB device under ±2 V was found to be only 77% of its original magnitude at ±1 V. Although extremely short response times of the order of a few ms have been realized in a PEDOT based device,[2] because of the many parameters such as cell dimensions, film morphology, mode and wavelength of measurement control kinetics, a direct comparison is therefore not possible. The cycling life of the PEDOT–PB device was measured at 0.0125 Hz under ±1 V at 632.8 nm (see ESI, Fig. 3†) and in the initial cycles for a 90% *T*-change, the color and bleach times were ~2.7 and 5.0 s. These increased to attain equivalent values (of 8.0 s) after 1200 cycles, and after 2500 cycles the coloring time increased slightly to 10 s, while the bleaching time of 8 s was retained. The optical modulation reduced to 86% of its original value after 1200 cycles and at the end of 2500 cycles, it shrunk to 74% of its original value, indicating that degradative reactions are not completely inhibited even whilst cycling within a relatively low potential range of +1 to −1 V.

Conclusions

PEDOT–PANI and PEDOT–PB devices encapsulating an ionic-liquid-based solid polymer electrolyte film of high transparency in the visible region and flexibility have been fabricated. Large coloration efficiencies were achieved for the PEDOT–PANI (η_{max} = 281 cm^2 C^{-1}, λ = 583 nm) and PEDOT–PB (η_{max} = 274 cm^2 C^{-1} at λ = 602 nm) devices, not at the highest inserted charge density, but at intermediate levels of charge intercalation. The optimum utilization of charge for the realization of large coloration efficiencies has been explained on the basis of the low magnitudes of charge transfer resistance, high polarization capacitance and fast ion-transport through the bulk of the film, during the reduction of PEDOT in both devices. Redox propagation in inorganic PB differed significantly from that of the organic PANI and PEDOT electrodes. The reductive charge transfer resistance and the polarization capacitance (under all biasing conditions) for PB were found to be unusually higher and lower, respectively, in comparison to the organic electrodes. Higher leakage currents have been shown to be responsible for the faster coloration kinetics in both devices and the reversibility of the dark to transparent and transparent to dark hues has been demonstrated for 2500 cycles for the PEDOT–PB device. The investigations on the electroactivity of the functional electrodes of electrochromic devices presented herein are expected to have a profound impact on the way cell architectures are conceived and evaluated by electrochemical probes.

Acknowledgements

Authors (S. Bhandari and A. Awadhia) thank UGC and CSIR for research fellowships. We thank NPL for financial support. We thank Director, NPL and Dr S.T. Lakshmikumar for encouragement and guidance.

References

1 A. A. Argun, P.-H. Aubert, B. C. Thompson, I. Schwendeman, C. L. Gaupp, J. Hwang, N. J. Pinto, D. B. Tanner, A. G. MacDiarmid and J. R. Reynolds, *Chem. Mater.*, 2004, **16**, 4401.
2 S. I. Cho, D. H. Choi, S.-H. Kim and S. B. Lee, *Chem. Mater.*, 2005, **17**, 4564.
3 L. B. Groenendaal, F. Jonas, D. Freitag, H. Pielartzik and J. R. Reynolds, *Adv. Mater.*, 2000, **12**, 481.
4 G. Li and P. G. Pickup, *Phys. Chem. Chem. Phys.*, 2000, **2**, 1255.
5 S. L. Cho and S. B. Lee, *Acc. Chem. Res.*, 2008, **41**, 699.
6 S. Bhandari, M. Deepa, A. K. Srivastava, C. Lal and Rama Kant, *Macromol. Rapid Commun.*, 2008, **29**, 1959.
7 T.-H. Lin and K.-C. Ho, *Sol. Energy Mater. Sol. Cells*, 2006, **90**, 506.
8 T.-S. Tung and K.-C. Ho, *Sol. Energy Mater. Sol. Cells*, 2006, **90**, 521.
9 P. M. S. Monk, R. J. Mortimer and D. R. Rosseinsky, in *Electrochromism and Electrochromic Devices*, Cambridge University Press, 2007, 25.
10 D. M. DeLongchamp and P. T. Hammond, *Chem. Mater.*, 2004, **16**, 4799.
11 A. Watanabe, K. Mori, Y. Iwasaki, Y. Nakamura and S. Niizuma, *Macromolecules*, 1987, **20**, 1793.
12 R. J. Mortimer and J. R. Reynolds, *J. Mater. Chem.*, 2005, **15**, 2226.
13 M. Deepa, S. Ahmad, K. N. Sood, J. Alam, S. Ahmad and A. K. Srivastava, *Electrochim. Acta*, 2007, **52**, 7453.
14 D. R. MacFarlane, M. Forsyth, P. C. Howlett, J. M. Pringle, J. Sun, G. Annat, W. Neil and E. I. Izgorodina, *Acc. Chem. Res.*, 2007, **40**, 1165.
15 A. S. Vuk, V. Jovanovski, A. P. Villard, I. Jerman and B. Orel, *Sol. Energy Mater. Sol. Cells*, 2008, **92**, 126.
16 W. Lu, A. G. Fadeev, B. Qi and B. R. Mattes, *J. Electrochem. Soc.*, 2004, **151**, H33.
17 W. Lu, A. G. Fadeev, B. Qi, E. Smela, B. R. Mattes, J. Ding, G. M. Spinks, J. Mazurkiewicz, D. Zhou, G. G. Wallace, D. R. MacFarlane, S. A. Forsyth and M. Forsyth, *Science*, 2002, **297**, 983.
18 W. Lu, B. R. Mattes, A. G. Fadeev and B. Qi, *US Pat.* 6 667 825 B2, 2003.
19 J. D. Stenger-Smith, C. K. Webber, N. Anderson, A. P. Chafin, K. Zong and J. R. Reynolds, *J. Electrochem. Soc.*, 2002, **149**, A973.
20 M. Deepa, S. Bhandari and Rama Kant, *Electrochim. Acta*, 2009, **54**, 1292.
21 S. Bhandari, M. Deepa, S. Singh, G. Gupta and Rama Kant, *Electrochim. Acta*, 2008, **53**, 3189.
22 M. Deepa, S. Bhandari, M. Arora and Rama Kant, *Macromol. Chem. Phys.*, 2008, **209**, 137.
23 S. Bhandari, M. Deepa, A. K. Srivastava and Rama Kant, *J. Nanosci. Nanotechnol.*, 2008, DOI: 10.1166/jnn.2008.050.
24 D. DeLongchamp and P. T. Hammond, *Adv. Mater.*, 2001, **13**, 1455.
25 T. Kobayashi, H. Yoneyama and H. Tamura, *J. Electroanal. Chem.*, 1984, **161**, 419.
26 S. Shreepathi and R. Holze, *Chem. Mater.*, 2005, **17**, 4078.
27 A. G. MacDiarmid, B. D. Humphrey and W.-S. Huang, *J. Chem. Soc., Faraday Trans. 1*, 1986, **82**, 2385.
28 M. Lapkowski, K. Berrada, S. Quillard, G. Louran, S. Lefrant and A. Pron, *Macromolecules*, 1995, **28**, 1233.
29 H. J. Ahonen, J. Lukkari and J. Kankare, *Macromolecules*, 2000, **33**, 6787.
30 H. Xia and Q. Wang, *Chem. Mater.*, 2002, **14**, 2158.
31 A. Kumar, D. M. Welsh, M. C. Morvant, F. Piroux, K. A. Abboud and J. R. Reynolds, *Chem. Mater.*, 1998, **10**, 896.
32 R. J. Mortimer and D. R. Rosseinsky, *J. Chem. Soc., Dalton Trans.*, 1984, 2059.
33 C. L. Gaupp, D. M. Welsh, R. D. Rauh and J. R. Reynolds, *Chem. Mater.*, 2002, **14**, 3964.
34 M. Fabretto, T. Vaithianathan, C. Hall, P. Murphy, P. C. Innis, J. Makurkiewicz and G. Wallace, *Electrochem. Commun.*, 2007, **9**, 2032.

35 R. D. Rauh, F. Wang, J. R. Reynolds and D. L. Meeker, *Electrochim. Acta*, 2001, **46**, 2023.
36 E. A. R. Duek, M.-A. DePaoli and M. Mastragostino, *Adv. Mater.*, 1992, **4**, 287.
37 R. Vergaz, D. Barrios, J. M. S. Pena, C. Marcos, C. Pozo and J. A. Pomposo, *Sol. Energy Mater. Sol. Cells*, 2008, **92**, 1071.
38 J. Bobacka, A. Lewenstamp and A. Ivaska, *J. Electroanal. Chem.*, 2000, **489**, 17.
39 J. R. Macdonald, in *Impedance Spectroscopy Emphasizing Solid Materials and Systems*, Wiley-Interscience, 1987.
40 M. Deepa, A. Awadhia, S. Bhandari and S. L. Agrawal, *Electrochim. Acta*, 2008, **53**, 7266.